Ion Thermal Decoupling and Species Separation in Shock-Driven Implosions

Hans G. Rinderknecht, M. J. Rosenberg, C. K. Li, N. M. Hoffman, G. Kagan, A. B. Zylstra, H. Sio, J. A. Frenje, M. Gatu Johnson, F. H. Séguin, R. D. Petrasso, P. Amendt, C. Bellei, S. Wilks, J. Delettrez, V. Yu. Glebov, C. Stoeckl, T. C. Sangster, D. D. Meyerhofer, and A. Nikroo

Phys. Rev. Lett. **114**, 025001 — Published 14 January 2015

DOI: 10.1103/PhysRevLett.114.025001

Ion Thermal Decoupling and Species Separation in Shock-Driven Implosions

Hans G. Rinderknecht,[1,*] M.J. Rosenberg,[1] C.K. Li,[1] N. M. Hoffman,[2] G. Kagan,[2] A.B. Zylstra,[1] H. Sio,[1] J.A. Frenje,[1] M. Gatu Johnson,[1] F.H. Séguin,[1] R.D. Petrasso,[1] P. Amendt,[3] C. Bellei,[3] S. Wilks,[3] J. Delettrez,[4] V. Yu. Glebov,[4] C. Stoeckl,[4] T.C. Sangster,[4] D.D. Meyerhofer,[4] and A. Nikroo[5]

[1]*Plasma Science & Fusion Center*
Massachusetts Institute of Technology, Cambridge, Massachusetts 02139 USA
[2]*Los Alamos National Laboratory, Los Alamos, NM 87545*
[3]*Lawrence Livermore National Laboratory, Livermore, California 94550*
[4]*Laboratory for Laser Energetics, Rochester, New York 14623*
[5]*General Atomics, San Diego, California 92121*

Anomalous reduction of the fusion yields by 50% and anomalous scaling of the burn-averaged ion temperatures with the ion-species fraction has been observed for the first time in D^3He-filled shock-driven inertial confinement fusion implosions. Two ion kinetic mechanisms are used to explain the anomalous observations: thermal decoupling of the D and ^{3}He populations and diffusive species separation. The observed insensitivity of ion temperature to varying deuterium fraction is shown to be a signature of ion thermal decoupling in shock-heated plasmas. The burn-averaged deuterium fraction calculated from the experimental data demonstrates a reduction in the average core deuterium density, as predicted by simulations that use a diffusion model. Accounting for each of these effects in simulations reproduces the observed yield trends.

In Inertial Confinement Fusion (ICF), targets are imploded to generate a high-density, high-temperature environment where fusion can occur.[1, 2] In the current ignition design, four weak shocks compress the cryogenic deuterium-tritium (DT) fuel, then combine into a single strong shock with Mach number ∼10-50 in the central gas, a DT-vapor with initial density 0.3 mg/cc.[3] Convergence of this shock at the implosion's center sets the initial entropy of the central plasma "hotspot" and generates a brief period of fusion production ("shock-bang"). The rebounding shock strikes the imploding fuel, beginning the hotspot compression that generates the main period of nuclear production ("compression burn"). Understanding the evolution of the plasma during the shock transit phase is fundamentally important for achieving ICF ignition, as this sets the initial conditions for hotspot formation, compression, ignition and burn.[4]

The simulations used to design ICF experiments generally assume a single average-ion hydrodynamic framework. The equations of motion for a single ion-species plasma are solved iteratively to model the implosion. Multiple ion species are not treated separately: the ion mass and charge are set as a weighted average of the individual species. Recent experimental and theoretical work has questioned the validity of the average-ion assumption.[5–15] Anomalous reduction of the compression-phase nuclear yield has been observed in implosions filled with multiple fuel species, such as deuterium-helium-3 (D^3He)[5], DT[6], and other combinations[7, 8]. Anomalous reduction of the shock yield has been ambiguous in these studies. Diffusive ion species separation driven by gradients in pressure[9], electric potential[10, 11], and temperature[12] is a potential cause of these observations.[13] Kinetic physics can impact the evolution and nuclear performance of multi-species plasmas in computational studies,[14, 15] although to the best of our knowledge no fully kinetic model is yet capable of simulating an entire ICF implosion.

The experiments described in this Letter demonstrate for the first time signatures of two multiple-ion kinetic physics effects in a series of D^3He-gas-filled, strongly-shocked implosions: thermal decoupling and diffusive separation of the ion populations. The observations suggest that these kinetic effects, which hydrodynamic simulations do not capture, have an important impact on ICF-relevant plasmas.

The experiments were performed at the 60-beam OMEGA laser facility.[16] Spherical capsules, 860 μm in diameter and made of 2.2 μm-thick glass,[17] were filled with various concentrations of D_2 and ^{3}He gas and imploded by an 0.6 ns, 23 TW laser pulse. These implosions mimic the density and shock strength in the ignition-target central gas. Notably, these shock-driven implosions are insensitive to hydrodynamic instability growth.[18–20] A high mass ablation rate and rapid ablation of the entire shell ("burn-through") stabilize ablation front instability growth early in the implosion; comparatively low convergence (∼3-5) and an unablated shell mass too small to substantially compress the fuel eliminate instability growth late in the implosion. 2D-hydrodynamic simulations of implosions with comparable shell mass and gas-fill density showed negligible instability growth at peak nuclear production.[19] Because of the minimal compression phase, the implosions produce primarily shock yield. The atomic deuterium fraction ($f_D \equiv n_D/(n_D + n_{^3He})$) of the gas fills ranged from 1 (pure deuterium) to 0.2 (^{3}He-rich), while maintaining a constant initial mass density of $\rho_0 = 0.4$ or 3.3 mg/cc. A constant ρ_0 maintains a constant Atwood number at the

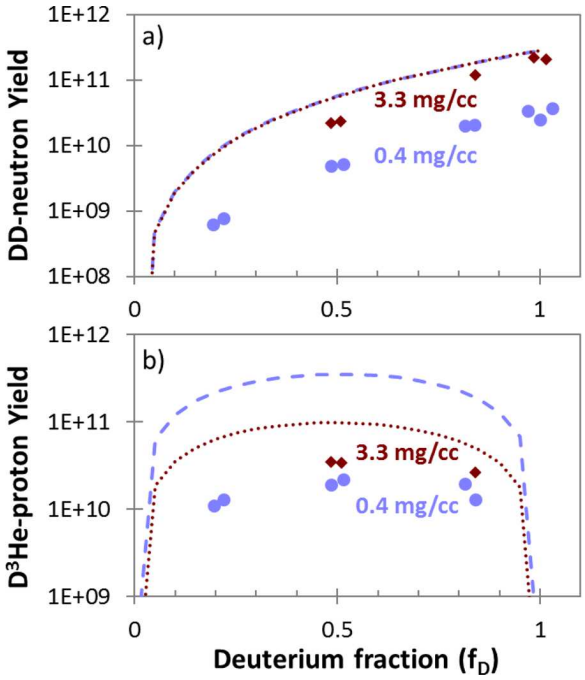

FIG. 1. (color online) Measured yields of a) DD-neutrons and b) D^3He-protons from implosions with initial fuel density of ρ_0 = 0.4 (blue) and 3.3 (red) mg/cc. For each ρ_0, the deuterium fraction (f_D) was varied. Points are artificially spread out in f_D for legibility. HYADES-simulated yield trends are shown for the low (dashed) and high (dotted) ρ_0.

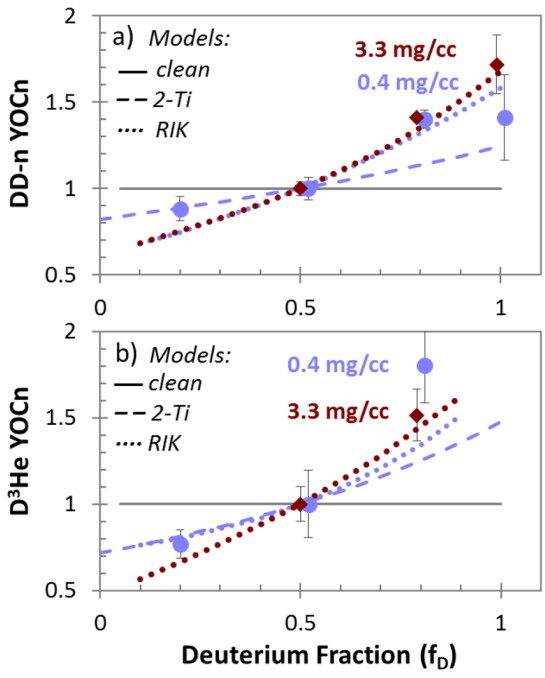

FIG. 2. (color online) Yields relative to 'clean' 1D-HYADES simulations, for a) DD-neutrons and b) D^3He-protons. Each dataset has been normalized to its value at $f_D = 0.5$. Modeled trends incorporating kinetic physics, such as decoupled ion temperatures ("2-Ti", dashed; low-ρ_0 only), and reduced ion kinetic models including ion diffusion ("RIK", dotted) match the measurements better than clean simulations (solid).

fuel-shell interface, which governs hydrodynamic mode growth and turbulent mix in the experiments.

Yields of DD-fusion neutrons (2.45 MeV) were measured using the neutron Time-of-Flight (nTOF) diagnostic suite.[21] Yields and spectra of D^3He-fusion protons (14.7 MeV) were recorded using the Charged Particle Spectrometers (CPS1 and CPS2) and Wedge-Range-Filter proton spectrometers (WRF)[22]. Burn-averaged ion temperatures were inferred from the nuclear spectral widths.[23, 24] Spatial burn profiles were measured by penumbral imaging of D^3He-protons and DD-protons (3.0 MeV).[25] 1D-radiation hydrodynamic simulations were performed using the code HYADES[26] for comparison to the observed values. Simulations were constrained using the the measured laser absorption fraction[29] of 57% and measured nuclear-bang times.[27, 28] Time-resolved self-emission x-ray images[30] confirmed the implosions were highly spherical.

The measured yields show anomalous trends relative to the hydrodynamically simulated values, as plotted in Figure 1. For each ρ_0, the yield drops relative to the predicted yield as the deuterium fraction is reduced from $f_D = 1$. (In subsequent figures, results from multiple implosions with the same nominal design are averaged.) The reduction in yield with decreasing ρ_0 was previously observed in a related experiment.[20]

To highlight the trend, the observed yield divided by the predicted yield is plotted in Figure 2, where each dataset has been normalized to the equimolar value ("Yield-over-clean normalized," or YOCn). The YOCn varies by 50% with f_D. These results provide the first conclusive experimental demonstration of a shock-yield anomaly with fuel ion fraction. The YOCn increase monotonically in the range $f_D > 0.2$, unlike the results for compression yield which showed a maximal reduction for equimolar D^3He and yield recovery approaching pure ^{3}He.[5][31] This trend cannot be explained by turbulent fuel-shell mix, since the Atwood number does not change with f_D. Two models including additional kinetic physics, decoupling of the D and ^{3}He ion temperatures ("2-Ti"), and species separation by ion diffusion (Reduced Ion Kinetic, or "RIK"), capture the observed trends, and will be discussed below.

The nuclear yields are given by

$$\begin{aligned} Y_{DD} &= \int \left(n_D^2/2\right) \langle\sigma v\rangle_{DD} dV dt \\ Y_{D^3He} &= \int n_D n_{^3He} \langle\sigma v\rangle_{D^3He} dV dt. \end{aligned} \quad (1)$$

Yields depend on the evolution of the Maxwellian-averaged fusion reactivities $\langle\sigma v\rangle_{DD,D^3He}$, which are strong functions of the ion temperature T_i. As shown in Figure 3, the measured burn-averaged ion temperatures $\langle T_i\rangle$ also demonstrate anomalous behavior compared to the average-ion simulations. In the low-density implo-

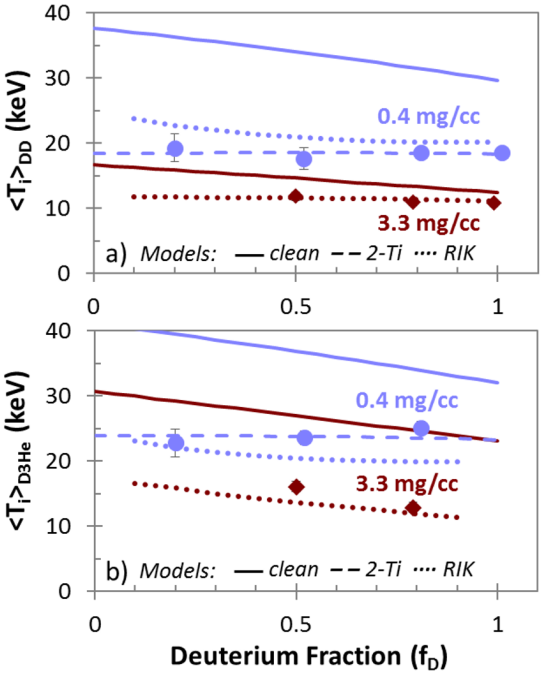

FIG. 3. (color online) Comparison of measured (points) and simulated (lines) burn-averaged ion temperatures $\langle T_i \rangle$ for the a) DD- and b) D^{3}He-fusion reactions. The 'clean' 1D-simulations (solid) predict an increased $\langle T_i \rangle$ with decreased f_D, which is not observed in the low-ρ_0 data. A model of decoupled D and ^{3}He ion temperatures in 1D-simulations ("2-Ti," dashed) reproduces the low-ρ_0 data. RIK simulations (dotted) model the absolute temperatures better than clean simulations.

sions, the measured $\langle T_i \rangle$ are roughly constant with deuterium fraction, whereas the 'clean' simulations predict increasing temperature for reduced f_D.[32]

This disagreement is a signature of thermal decoupling between the deuterium and helium-3. Shocks deliver different amounts of energy to the two ion species, depending on their charges and masses. Heating from collisional strong shocks scales with the ion mass ($T_i \propto m_i v_{sh}^2$, where v_{sh} is the shock velocity) whereas the energy delivered by electrostatic collisionless shocks scales with the ion charge ($T_i \propto Z_i \Delta\Phi_{sh}$, where Φ_{sh} is the electric potential). In either scenario, the ^{3}He ions receive more energy than the D, by a factor of 1.5 or 2, respectively. This difference persists for the thermal equilibration timescale, shown in Table I as calculated using the measured plasma conditions at shock burn.[33] Comparing the inter-species equilibration timescales to the measured burn durations, it is likely that ion temperatures are unequilibrated during shock burn in the low-density implosions.

The shock properties ($v_{sh}, \Delta\Phi_{sh}$) and the shocked deuterium- and ^{3}He-temperatures are expected to be constant for a fixed ρ_0. If the species do not equilibrate, the burn-averaged ion temperatures are therefore constant as well. This signature is observed in the low-density data in Figure 3. In contrast, the hydrodynamic simulations require a single ion temperature, which scales with the average-ion mass $\langle m_i \rangle = (3 - f_D)\, m_p$. The observed $\langle T_i \rangle$ indicate that multi-ion kinetic physics is important for thermal evolution in the low-ρ_0 experiments.

TABLE I. Thermal equilibration timescales ($\tau_{D/^3He}, \tau_{^3He/D}$) and thermalization timescales ($\tau_D, \tau_{^3He}$) in picoseconds for various ρ_0 and f_D.[33] Bolded values exceed the measured DD-burn duration τ_{burn} (full-width at half maximum).

Density (mg/cc)	f_D	Ion-ion equilibration time $\tau_{D/^3He}$	$\tau_{^3He/D}$	τ_D	$\tau_{^3He}$	τ_{burn}
0.4	0.2	**240**	**930**	**2730**	70	180
	0.5	**330**	**320**	**980**	90	180
	0.8	**890**	**190**	**600**	**250**	160
	1		140	**440**		160
3.3	0.5	120	130	**380**	40	180
	0.8	**240**	50	150	70	170
	1		40	120		170

To determine the effect of thermal decoupling on the yield, the low-ρ_0 simulations were post-processed with an empirical model that was fit to the measured $\langle T_i \rangle$. The D and ^{3}He temperatures were defined in terms of the simulated ion temperature (T_1) and f_D as:

$$T_{^3He} = T_D R_T = T_1 f_T \frac{R_T}{f_D + R_T(1 - f_D)}. \qquad (2)$$

where the ratio of temperatures $R_T (\equiv T_{^3He}/T_D)$ and the scalar f_T are free parameters. This formulation conserves the thermal energy in the plasma up to the scalar f_T. The effective temperatures for fusion reactivity and spectral $\langle T_i \rangle$ measurements were defined as $T_{eff,ij} = (m_i T_j + m_j T_i)/(m_i + m_j)$,[14] and $T_{spect,ij} = (m_i T_i + m_j T_j)/(m_i + m_j)$,[15] respectively. The best-fit of this model to 15 measured $\langle T_i \rangle$ from the low-ρ_0 experiments was $R_T = 1.3 \pm 0.1$, $f_T = 0.61 \pm 0.02$, and is shown in Figure 3. This model improves agreement with the observed yield trends, as shown in Figure 2. No reasonable fit to the high-ρ_0 $\langle T_i \rangle$ data could be found using this model, suggesting that thermal decoupling is not a dominant effect. This is not surprising given the much shorter equilibration times in Table I.

Interestingly, the long ion-ion equilibration times at shock convergence imply that neither ion species is well-described as a thermal distribution. Thermalization and collisional timescales are comparable, implying that decoupled plasmas are collisionless. As noted earlier, a collisionless shock delivers less energy to the D than to the ^{3}He. While this condition holds, long equilibration times must reduce the average deuteron energy compared to the thermal expectation. This directly reduces the average center-of-mass energy for D-D collisions, and therefore the inferred $\langle T_i \rangle$ and the yield. Fully kinetic simulations incorporating Monte Carlo fusion production are required to evaluate fully the effects of non-thermal ion

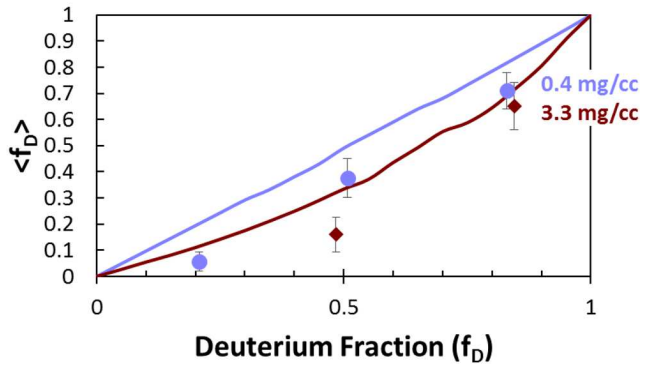

FIG. 4. (color online) "Burn-averaged deuterium fraction" $\langle f_D \rangle$ evaluated from the experiments for low-density (blue) and high-density (red) implosions, compared to 1D-clean simulations (lines). Simulated values for $\langle f_D \rangle$ differ slightly from the fuel f_D due to differences in the D^3He- and DD-reactivity. Reduction of the deuterium in the core prior to burn is inferred for all implosions.

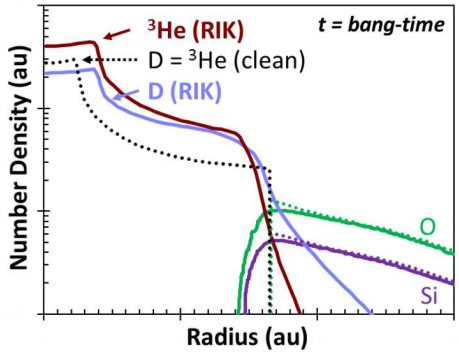

FIG. 5. (color online) Density profiles near bang-time for an equimolar D^3He implosion with $\rho_0 = 3.3$ mg/cc, comparing 1D-average-ion 'clean' simulations (dotted) with simulations including reduced ion kinetic models of ion diffusion, ion thermal conduction, and tail-ion loss (solid). The deuterium (blue) diffuses to larger radii and ^3He (red) is concentrated in the core, such that at peak burn $f_D = 0.33$. The RIK simulations reproduce the observed yields.

distributions on the measured data.

Separation of the ion species by diffusion provides an additional explanation for the observed yield trends.[9, 11] Although the ion species fraction during burn is not measured directly, quantities proportional to the ion densities can be inferred by inverting Equations 1. The yield, $\langle T_i \rangle$, burn duration, and radius containing 50% of the nuclear burn (r_{50}) are measured for both the DD and D^3He reactions. Using these quantities, the burn-averaged density products can be calculated for ion species i,j as:

$$\langle n_i n_j \rangle = \left(\frac{(1+\delta_{ij})Y}{\langle \sigma v \rangle (\langle T_i \rangle)(4\pi r_{50}^3/3)\tau_{burn}} \right)_{ij} \quad (3)$$

where quantities are measured for the i-j fusion reaction, and δ_{ij} is the Kronecker delta. The burn-averaged deuterium fraction is then defined as $\langle f_D \rangle = (1 + \langle n_D n_{^3He} \rangle / \langle n_D^2 \rangle)^{-1}$. This definition is not expected to be identical to the initial gas f_D, as the D^3He and DD reactions are weighted differently in the implosion. However, it is proportional to ion species fraction to first order, and can be compared directly to simulations, as shown in Figure 4. The measured $\langle f_D \rangle$ are lower than the predicted values, implying that species separation significantly perturbs the ion distributions prior to bang-time. Comparing the high-ρ_0 equimolar result to the simulated trend, the fuel deuterium fraction at bang-time is reduced from $f_D = 0.5$ to 0.28 ± 0.10.

Using a 1D-radiation hydrodynamic simulation incorporating a model of plasma ion kinetic transport and other reduced ion kinetic (RIK) models,[34] the effect of species separation in these experiments was investigated. RIK parameters were calibrated to provide the best-fit to five observables in comparable equimolar high- and low-ρ_0 implosions from a related experiment.[20] These high- and low-density models were applied while varying f_D to obtain the yield and temperature trends in Figures 2 and 3. The RIK simulations captured the yield trend for the high-density experiments while also matching the measured $\langle T_i \rangle$. A radial profile of the ion species densities at bang-time from the equimolar, high-ρ_0 RIK simulation is shown in Figure 5. In this simulation, ion diffusion had reduced f_D in the core from 0.5 to 0.33 prior to shock-bang, in agreement with the results in Figure 4. The deuterium was redistributed to the outer regions of the fuel, where it fuses less efficiently due to lower temperatures and admixture with shell material.

The RIK models include flux-limited ion thermal conduction, and account for Knudsen-layer reactivity reduction.[35] Due to these effects, the model closely matches the observed temperatures and yields. However, the RIK simulations do not capture the observed $\langle T_i \rangle$ trends for the low-ρ_0 data. This is not surprising, as the models do not include separate ion thermal distributions. More fundamentally, the RIK models are kinetic perturbations on bulk hydrodynamic evolution, which may not extend to describe the fully kinetic behavior implied by thermal decoupling. This discrepancy supports ion thermal decoupling as a dominant physical effect in the low-density regime.

In summary, a series of D^3He-gas-filled shock-driven implosions have demonstrated anomalously low yields and burn-averaged ion temperatures as deuterium fraction is reduced. Kinetic processes associated with multiple ion species are proposed to explain these anomalies. Ion-ion thermalization times in excess of the burn duration suggest that the preferential heating of ^3He ions by the shock subsists through the burn, producing the observed 'flat' trends in the low-density $\langle T_i \rangle$. A post-processed 1D-radiation hydrodynamic simulation allow-

ing for different D and ^{3}He temperatures recaptures the observed $\langle T_i \rangle$ and yield trends. The burn-averaged deuterium fraction inferred from measurements was lower than expected in all experiments: the first direct evidence of species separation in ICF implosions. Simulations including ion diffusion demonstrate significant reduction of the core deuterium fraction prior to bang-time, and produce a yield trend similar to observations. The experimental results suggest that ion kinetic effects play an important role in the low-density, strongly-shocked plasma of the incipient hotspot in ICF ignition implosions. These effects may impact the hotspot adiabat, and species separation seeded prior to shock-bang may persist until peak compression and burn. Fully kinetic simulations will be required to simultaneously capture the impact of non-thermalized ions and species separation, to better understand how these effects impact ICF ignition designs.

The authors thank R. Frankel and E. Doeg for contributing to the processing of CR-39 data used in this work, as well as the OMEGA operations crew for their help in executing these experiments. This work is presented in partial fulfillment of the first author's PhD thesis and supported in part by US DoE/NNSA (Grant No. DE-NA0001857), FSC (No. 415023-G), NLUF (No. DE-NA0002035), LLE (No. 415935-G), and LLNL (No. B600100).

* hgr@mit.edu

[1] J. Nuckolls, L. Wood, A. Thiessen, and G. Zimmerman, Nature **239**, 139 (1972).
[2] J. Lindl, Phys. Plasmas **2**, 3933 (1995).
[3] S. W. Haan *et al.*, Phys. Plasmas **18**, 051001 (2011).
[4] W. H. Goldstein, *Science of Fusion Ignition on NIF*, Tech. Rep. LLNL-TR-570412 (Lawrence Livermore National Laboratory, 2012).
[5] J. R. Rygg *et al.*, Phys. Plasmas **13**, 052702 (2006).
[6] D. T. Casey *et al.*, Phys. Rev. Lett. **108**, 075002 (2012).
[7] H. W. Herrmann *et al.*, Phys. Plasmas **16**, 056312 (2009).
[8] D. C. Wilson *et al.*, J. Phys. Conf. Ser. **112**, 022015 (2008).
[9] P. Amendt, O. L. Landen, H. F. Robey, C. K. Li, and R. D. Petrasso, Phys. Rev. Lett. **105**, 115005 (2010).
[10] P. Amendt, S. C. Wilks, C. Bellei, C. K. Li, and R. D. Petrasso, Phys. Plasmas **18**, 056308 (2011).
[11] G. Kagan and X.-Z. Tang, Phys. Plasmas **19**, 082709 (2012).
[12] G. Kagan and X.-Z. Tang, Phys. Lett. A **378**, 1531 (2014).
[13] P. Amendt, C. Bellei, S. Wilks, C. K. Li, R. D. Petrasso, and H. G. Rinderknecht, Phys. Rev. E **(to be submitted)**.
[14] C. Bellei, H. Rinderknecht, A. Zylstra, M. Rosenberg, H. Sio, C. K. Li, R. Petrasso, S. C. Wilks, and P. A. Amendt, Phys. Plasmas **21**, 056310 (2014).
[15] A. Inglebert, B. Canaud, and O. Larroche, EPL (Europhysics Letters) **107**, 65003 (2014).
[16] T. R. Boehly *et al.*, Opt. Commun. **133**, 495 (1997).
[17] Glass density is 2.15 g/cm^3.
[18] C. Bayer, M. Bernard, D. Billon, M. Decroisette, D. Galmiche, D. Juraszek, J. Launspach, D. Meynial, and B. Sitt, Nucl. Fusion **24**, 573 (1984).
[19] H. G. Rinderknecht *et al.*, Phys. Rev. Lett. **112**, 135001 (2014).
[20] M. J. Rosenberg *et al.*, Phys. Rev. Lett. **112**, 185001 (2014).
[21] V. Y. Glebov, C. Stoeckl, T. C. Sangster, S. Roberts, G. J. Schmid, R. A. Lerche, and M. J. Moran, Rev. Sci. Instrum. **75**, 3559 (2004).
[22] F. H. Séguin *et al.*, Rev. Sci. Inst. **74** (2003).
[23] H. Brysk, Plasma Physics **15**, 611 (1972).
[24] L. Ballabio, J. Källne, and G. Gorini, Nucl. Fus. **38**, 1723 (1998).
[25] F. H. Séguin *et al.*, Phys. Plasmas **13**, 082704 (2006).
[26] J. T. Larsen and S. M. Lane, J. Quant. Spectrosc. Ra. **51**, 179 (1994).
[27] R. A. Lerche, D. W. Phillion, and G. L. Tietbohl, Rev. Sci. Instrum. **66**, 933 (1995).
[28] J. A. Frenje *et al.*, Phys. Plasmas **11**, 2798 (2004).
[29] W. Seka, H. A. Baldis, J. Fuchs, S. P. Regan, D. D. Meyerhofer, C. Stoeckl, B. Yaakobi, R. S. Craxton, and R. W. Short, Phys. Rev. Lett. **89**, 175002 (2002).
[30] D. K. Bradley, P. M. Bell, O. L. Landen, J. D. Kilkenny, and J. Oertel, Rev. Sci. Instrum. **66**, 716 (1995).
[31] Experiments with ρ_0 = 1.5 mg/cc and a 1 ns, 23 TW laser pulse showed a flattening of YOCn in the limit f_D = 0.07, rather than a continuous decay.
[32] The disagreement in the absolute value of yields and $\langle T_i \rangle$ between measurements and 1D-simulations is comparable to that observed in Ref. [20].
[33] J. D. Huba, "NRL Plasma Formulary," Naval Research Laboratory, Washington, D.C. (2006).
[34] N. M. Hoffman *et al.*, (to be published).
[35] K. Molvig, N. M. Hoffman, B. J. Albright, E. M. Nelson, and R. B. Webster, Phys. Rev. Lett. **109**, 095001 (2012).